Investigation of a Cable-Driven Parallel Mechanism for Interaction with a Variety of Surfaces, Applied to the Cleaning of Free-Form Buildings

K.H.J. Voss, V. van der Wijk and J.L. Herder

Abstract In this paper, the capability of a specific cable-driven parallel mechanism to interact with a variety of surfaces is investigated. This capability could be of use in for example the cleaning of large building surfaces. A method is presented to investigate the workspace for which the cables do not interfere and a surface interaction force can be generated. This method takes into account the influence of cable mass. As an example, this method is used for the design of a mechanism with a workspace conform to the dimensions of a typical building facade. The mechanism is concluded to be feasible as long as there is room to locate the pulleys at an adequate distance from the surface.

Key words: Cable-driven parallel mechanism, cable interference, workspace, cable mass influence, surface interaction

1 Introduction

The cleaning of building surfaces, especially large ones, is a challenging task because of the difficulty in reaching them. With the increasing number of buildings with free-form architecture, so called 'blobitecture', this task has become even more challenging, and sometimes even impossible to do with conventional equipment such as suspended platforms [13]. Another problem is that conventional cleaning is expensive, because of the considerable amount of human labor involved [4] and the necessary adaptations to the building to make it cleanable.

For the cleaning of glass surfaces, several automated devices have been proposed and developed, e.g. [3, 4]. However, they still require human labor or they are only applicable to a single surface or a limited number of simple surfaces. The current problem is therefore that a cost-effective automated device that can interact with a wide variety of large and small, straight and curved surfaces is still to be found.

K.H.J. Voss · V. van der Wijk · J.L. Herder
Department of Mechanical Automation and Mechatronics, Faculty of Engineering Technology, University of Twente, 7500 AE Enschede, The Netherlands, e-mail: k.h.j.voss@student.utwente.nl

J. Lenarčič, M. Husty (eds.), *Latest Advances in Robot Kinematics*,
DOI 10.1007/978-94-007-4620-6_33,

Cable Driven Parallel Mechanisms (CDPMs) are known to have several advantages: they have a large workspace to mass ratio, they are easy to reconfigure and they are relatively cheap [5, 9]. Therefore these mechanisms have a large potential for the cost-effective interaction with a wide variety of surfaces. However, to the authors best knowledge, the investigation of these mechanisms for this purpose is unknown.

The goal of this paper is therefore to propose a CDPM for the purpose of interaction with a variety of large surfaces.

The paper is structured as follows. Firstly, the device configuration is presented. Secondly, the method for the determination of the workspace in order to investigate its feasibility for interaction with large free-form surfaces is presented. In this method cable interferences, the influence of cable mass and the ability to provide a surface interaction force are taken into account. The method is applied to an example, yielding numerical results that are then discussed. The control of the device and the actual cleaning process are not treated in this paper.

2 Mechanism Configuration and Definitions

Figure 1 shows the configuration of an eight cable CDPM. It consists of actuated winches located at points $\mathrm{A_i}$. For the application on a building, these winches can be mounted on the ground, the roof or on beams at a distance from the surface. The winches are connected by cables to a mobile platform at $\mathrm{B_i}$. An end-effector (e.g. a cleaning head [2]) can be located at H. F is the fixed frame and M is the mobile frame attached to the platform. Vectors $\mathbf{A_{i,F}}$ describe the location of points $\mathrm{A_i}$ in F, vectors $\mathbf{B_{i,M}}$ describe the location of $\mathrm{B_i}$ in M.

The three translational degrees of freedom (DOFs) of the platform are described by the vector $\mathbf{r}$ directed from the origin of F to the origin of M. The three rotational DOFs of the platform are defined by a rotation about the y-, x- and z-axis of F respectively, contained in vector $\theta = [\theta_x, \theta_y, \theta_z]^{\mathrm{T}}$. This rotation from F to M is described by a rotation matrix $\mathbf{R}(\theta) = \mathbf{R_z}(\theta_z)\mathbf{R_x}(\theta_x)\mathbf{R_y}(\theta_y)$, where the latter three matrices are elementary rotation matrices. The pose is defined as $\mathbf{x} = [\mathbf{r}^{\mathrm{T}}, \theta^{\mathrm{T}}]^{\mathrm{T}}$, which thus includes all DOFs. The surface to be interacted with lies within quadrilateral $\mathrm{A_5A_6A_7A_8}$ with possible features in y_F direction.

There is actuation redundancy because there are eight actuated cables actuating six DOFs; The seventh cable is necessary to keep tension in the cables, the eighth is added to achieve a proper workspace.

Surfaces conform those usually found on buildings have large dimensions in two directions, and also some smaller features in the third direction. However, the workspace of a CDPM usually has fairly equal dimensions in all directions (e.g. [1, 11]). In this paper it will be shown that the presented CDPM has the proper workspace with one small edge and two long edges, which could make it applicable on the set of mentioned surfaces. Within this workspace, the cables are always free of interference and an interaction force on the surface can be produced.

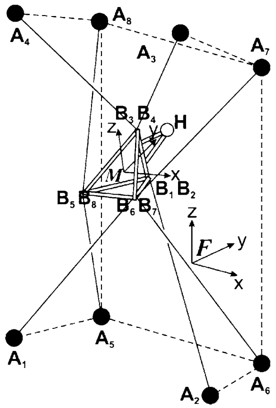

Fig. 1 CDPM configuration.

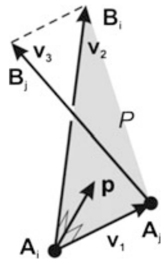

Fig. 2 Cable pair.

3 Method

To generate a workspace in which cables do not interfere, the interference needs to be detected. This needs to be done in such a way that the result is also valid for cables that sag due to their mass and that it is implementable in the method for calculating a wrench feasible workspace, which is explained later. This made existing methods to calculate cable interferences (e.g. [8, 10]) insufficient. Therefore a new method is developed specifically for this configuration.

Instead of investigating the interference between each possible pair of cables and also the mobile platform, a simplifying observation can be made. Namely, interference will always occur between cables in one of the pairs of cables 1-5, 2-6, 3-7 and 4-8, prior to any interference between cables belonging to different pairs or between a cable and the mobile platform. Therefore, interference is tested solely between two cables in one of these pairs. E.g. a rotation of the pose in Fig. 1 around the z_F axis will result in interference occurring first in pair 1-5 or 4-8.

Figure 2 shows a pair of cables i and j in a state of no interference. Plane P with normal vector $\mathbf{p}$ is spanned by $\mathbf{v_1}$ from pulley $\mathrm{A_i}$ to $\mathrm{A_j}$ and by $\mathbf{v_2}$ from $\mathrm{A_i}$ along cable i. The cables in this pair are defined to interfere if cable j ($\mathbf{v_3}$) lies in or on the other side of P, because it will then have crossed cable i. This is the case if $\angle(\mathbf{p}, \mathbf{v_3}) \geq 90°$, or in terms of the vectors $\mathbf{v_i}$:

$$\det([\mathbf{v_1}, \mathbf{v_2}, \mathbf{v_3}]) \leq 0. \tag{1}$$

Eq. (1) is still based on an assumption of massless, straight cables. To account for mass effects, i.e. sag of the cables, a distance margin d_{mar} is introduced. Should the minimal distance d_{min} between two straight cables fall below d_{mar}, the sagged cables are defined to interfere, see Eq. (2).

$$d_{\min} = \left| \mathbf{v_1} \cdot \frac{\mathbf{v_2} \times \mathbf{v_3}}{\|\mathbf{v_2} \times \mathbf{v_3}\|} \right| = \left| \frac{\det([\mathbf{v_1}, \mathbf{v_2}, \mathbf{v_3}])}{\|\mathbf{v_2} \times \mathbf{v_3}\|} \right| < d_{\mathrm{mar}}. \tag{2}$$

Instead of testing for interference by evaluating Eqs. (1) and (2), they can be combined in Eq. (3), allowing for a single equation to test for interference.

$$\frac{\det([\mathbf{v_1}, \mathbf{v_2}, \mathbf{v_3}])}{\|\mathbf{v_2} \times \mathbf{v_3}\|} < d_{\mathrm{mar}}. \tag{3}$$

To determine a proper d_{mar}, the sagged state of the cables will be compared to the state with straight cables. The method to calculate the sagged state is adapted from [7, 12], in which the location of one end of a cable in a local x-z plane with the other end clamped at $(0,0)$ is given by Eqs. (4) and (5).

$$x_{\mathrm{end}} = \frac{F_x L_0}{EA_0} + \frac{|F_x|}{\rho_0 g}\left(\operatorname{asinh}\left(\frac{F_z}{F_x}\right) - \operatorname{asinh}\left(\frac{F_z - \rho_0 g L_0}{F_x}\right)\right), \tag{4}$$

$$z_{\mathrm{end}} = \frac{F_z L_0}{EA_0} - \frac{\rho_0 g L_0^2}{2EA_0} + \frac{1}{\rho_0 g}\left(\sqrt{F_x^2 + F_z^2} + \sqrt{F_x^2 + (F_z - \rho_0 g L_0)^2}\right). \tag{5}$$

For a given pose of the mobile platform, x_{end} and z_{end} can be calculated for each cable. Young's modulus E, cable cross-sectional area A_0, linear density ρ_0 and gravitational acceleration g are assumed to be known. The forces F_x and F_z at the end and the sagged cable length L_0 are to be calculated, which are three unknowns for two equations. Therefore there are $2m$ equations for $3m$ unknowns for an n-DOF, m-cable device. Then, with static equilibrium providing an additional n equations, the equations are solvable for an $n = m$ CDPM, as was done in [7, 12]. However, an $n = m - 2$ CDPM like the one investigated here has two extra free variables. These free variables are used in the adapted method presented here.

At first, suppose that the cables are massless and therefore straight. Then Eq. (6) [1] shows how 6×8 wrench matrix $\mathbf{W_M}$ relates the cable tension forces gathered in 8×1 vector $\mathbf{t}$ to the forces and torques (i.e. wrench), gathered in 6×1 wrench vector $\mathbf{f_M}$ in M.

$$\mathbf{W_M t} = \begin{bmatrix} \mathbf{u}_{1,\mathbf{M}} & \cdots & \mathbf{u}_{8,\mathbf{M}} \\ \mathbf{B}_{1,\mathbf{M}} \times \mathbf{u}_{1,\mathbf{M}} & \cdots & \mathbf{B}_{8,\mathbf{M}} \times \mathbf{u}_{8,\mathbf{M}} \end{bmatrix} \mathbf{t} = \mathbf{f_M}, \quad \mathbf{u}_{\mathbf{i},\mathbf{M}} = \frac{\mathbf{l}_{\mathbf{i},\mathbf{M}}}{\|\mathbf{l}_{\mathbf{i},\mathbf{M}}\|} \tag{6}$$

The unknowns for a given pose $\mathbf{x}$ and a given external force vector $\mathbf{f_M}$ are calculated using a four step method. The first step is to solve the linear programming equation of Eq. (7) [6] with cable tensions $\mathbf{t}$ between specified bounds. $\mathbf{c} = -\mathbf{1}$ to find maximal valid cable tensions, which results in low sag.

$$\min_{\mathbf{t}} \mathbf{c}^{\mathrm{T}} \mathbf{t} \text{ such that } \mathbf{W_M t} = \mathbf{f_M}, \ \mathbf{t} \in [\mathbf{t}_{\mathrm{low}}, \mathbf{t}_{\mathrm{high}}]. \tag{7}$$

The second step is to solve the system of Eqs. (4) and (5) and equilibrium for the eight cables simultaneously. The initial values of F_x and F_z for each cable are calculated from the $\mathbf{t}$ found with Eq. (7). The initial values of the L_0 are $\|\mathbf{L_{i,M}}\| = \|\mathbf{A_{i,M}} - \mathbf{B_{i,M}}\|$.

The found solution for $\mathbf{t}$ is not unique because of the free variables, but starting from this solution, these variables can be used to affect the sag of all cables so that they stay below a pre-defined limit $\delta_{\max}$. This limit is defined by Eq. (8), and if this equation is not true, step three is performed.

$$\forall i \in [1,2,\ldots,8]: \ \delta_i \leq \delta_{\max}, \ \text{where } \delta_i = \frac{L_{0,i} - \|\mathbf{l_i}\|}{\|\mathbf{l_i}\|}. \tag{8}$$

Step three is to add Eq. (9) to the system of equations and solve it again, where i is the number of the cable with the largest δ_i, F_p is the solution for F_z for this cable and $\alpha > 1$. The effect is that the F_z for the cable with the most sag is increased, which reduces its δ_i. Step three is repeated until Eq. (8) is valid. $\delta_{\max}$ needs to be raised if this proves impossible.

$$F_{z,i} = \alpha F_p. \tag{9}$$

For step four, it is now possible to calculate the path of a sagged cable from $\mathrm{A_i}$ to $\mathrm{B_i}$ with [7, 12]. This allows minimal distances between the sagged cables to be calculated and the presence of interference to be investigated with a plot. By comparing these results at a number of poses for which Eq. (3) predicts interference, the optimal d_{mar} can be found.

Now that d_{mar} is known, the space that needs to be tested for interference is discretized into a finite number of poses. If for a specific grid point Eq. (3) is false for each pair of cables, it is considered that there is no interference and the corresponding pose is added to the interference free space (IFS).

In addition to being interference free, at a pose an adequate surface normal force also needs to be producible. This means that there should be equilibrium for an $\mathbf{f_M}$ in which a surface interaction is specified along the y_M direction and a gravity force is specified in the proper direction. This could be tested by checking whether the system of sag equations converges for this pose and this $\mathbf{f_M}$. However, a lack of convergence might also indicate a wrongly defined $\delta_{\max}$ or α and it is recommended to visually inspect the solution for a pose that does converge. This makes this approach infeasible and instead, a test for wrench feasibility with a method adapted from [6] to include the effects of cable mass is proposed.

A pose is wrench feasible if at this pose Eq. (6) can be satisfied with a $\mathbf{t} \in [\mathbf{t}_{\min}, \mathbf{t}_{\max}]$; this can be tested with [6]. Although this method is based on massless cables, the cable mass is accounted for in two ways. Firstly, the cable mass m_c given by $m_c = \rho_0 \sum_{i=1}^{8} \|\mathbf{l_i}\|$ is added to the platform mass m_p, resulting in a larger gravity force $\mathbf{f_M}$. Not just a part, but the entire mass of all eight cables is added, because the pulleys at the top need to lift this entire mass.

Secondly, the $\mathbf{t}_{\min}$ is determined in the same way as d_{mar} is determined: for a number of representative poses with sagged cables the cable tensions are calculated. The cable tensions that are found to be minimally necessary to keep Eq. (8) valid are the input for $\mathbf{t}_{\min}$. In [6] wrench feasibility is tested for pose intervals. To reduce

Table 1 Numerical values, all coordinates are in meters

$\mathbf{A_{1,F}}$	$[-30,-5,-50]^{\mathrm{T}}$	$\mathbf{A_{5,F}}$	$[-30,5,-50]^{\mathrm{T}}$	$\mathbf{B_{1,M}}$	$[0,3,-2]^{\mathrm{T}}$	$\mathbf{B_{5,M}}$	$[-3,-3,0]^{\mathrm{T}}$
$\mathbf{A_{2,F}}$	$[30,-5,-50]^{\mathrm{T}}$	$\mathbf{A_{6,F}}$	$[30,5,-50]^{\mathrm{T}}$	$\mathbf{B_{2,M}}$	$[0,3,-2]^{\mathrm{T}}$	$\mathbf{B_{6,M}}$	$[3,-3,0]^{\mathrm{T}}$
$\mathbf{A_{3,F}}$	$[30,-5,65]^{\mathrm{T}}$	$\mathbf{A_{7,F}}$	$[30,5,60]^{\mathrm{T}}$	$\mathbf{B_{3,M}}$	$[0,3,2]^{\mathrm{T}}$	$\mathbf{B_{7,M}}$	$[3,-3,0]^{\mathrm{T}}$
$\mathbf{A_{4,F}}$	$[-30,-5,65]^{\mathrm{T}}$	$\mathbf{A_{8,F}}$	$[-30,5,60]^{\mathrm{T}}$	$\mathbf{B_{4,M}}$	$[0,3,2]^{\mathrm{T}}$	$\mathbf{B_{8,M}}$	$[-3,-3,0]^{\mathrm{T}}$
$\mathbf{H_M}$	$[0,5,0]^{\mathrm{T}}$	ρ_0	0.24 kg/m	E	400 GPa	A_0	50 mm^2
m_p	250 kg	g	9.81 m/s2				

calculation time, here the IFS is used as an input grid of poses to test. The result is an interference free wrench feasible workspace (IFWFW).

4 Results

The method is applied to the configuration of Fig. 1 with the numerical values of Table 1. m_p is the mass of the platform; ρ_0, E and A_0 are consistent with commercially available fiber core wire rope. Using the discussed method, the table values were selected to make a good set for the cleaning of a building facade of 40×100 m with feature depths of 5 m.

$$\mathbf{f_M} = \left[[\mathbf{F_s} + \mathbf{F_g}]^{\mathrm{T}}, 0, 0, 0\right]^{\mathrm{T}}, \quad \mathbf{F_s} = [0, 100, 0]^{\mathrm{T}}, \quad \mathbf{F_g} = \mathbf{R}(\theta)^{\mathrm{T}}[0, 0, mg]^{\mathrm{T}} \tag{10}$$

The wrench vector $\mathbf{f_M}$ used in this analysis is given by Eq. (10). Herein, a surface interaction force of 100 N is defined in $+y_M$ direction. A force mg in $+z_F$ direction counteracts the gravity on the platform. $\mathbf{R}(\theta)^{\mathrm{T}}$ rotates this force to the mobile frame. $m = m_p$ for the sag analysis and $m = m_p + m_c$ for the wrench feasibility analysis. The rest of the forces and the torques are zero for equilibrium.

Using this force vector, the influence of cable mass is investigated for a number of poses to find a suitable d_{mar} and $\mathbf{t}_{\mathrm{min}}$. A $\delta_{\mathrm{max}} = 0.0005$ and $\alpha = 1.1$ were used for these investigations. Together with all entries of $\mathbf{t}_{\mathrm{high}}$ equal to 6 kN in Eq. (7) this resulted in maximal cable tensions of around 9.5 kN for the final solution of all poses of the sagged state. This corresponds to a safety factor of 4 for the used wire rope and will also be used as the $\mathbf{t}_{\mathrm{max}}$ for the wrench feasibility analysis. A d_{mar} of 0.35 m was concluded to be adequate. This occurred e.g. at pose $\mathbf{x} = [20, 0, 40, 19°, 0°, 20°]^{\mathrm{T}}$ where the cables 1 and 5 were observed to touch each other in sagged state, while Eq. (3) predicted a distance of 0.35 m. A cable tension of 1.6 kN insures that Eq. (8) is satisfied for each cable in each pose and therefore this is used as the $\mathbf{t}_{\mathrm{min}}$ for the wrench feasibility analysis.

Figure 3 shows the result of pulling the cables tight to make Eq. 8 valid for the pose $\mathbf{x} = [20, 0, 50, 0°, 0°, 0°]^{\mathrm{T}}$. Cable 5 had too much sag at first, which is illustrated by the dashed line. After pulling the cable tight, the cable was located along the solid line. This increased the minimal distance between Cable 1 and 5 from 0.48 m to 1.26 m, which shows how this method can increase the interference free space. Another effect of pulling tight is that the stiffness added by Cable 5 to the

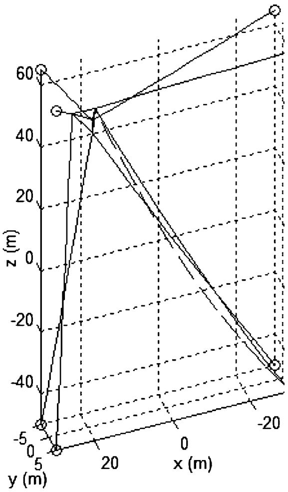

Fig. 3 Sagged cable states.

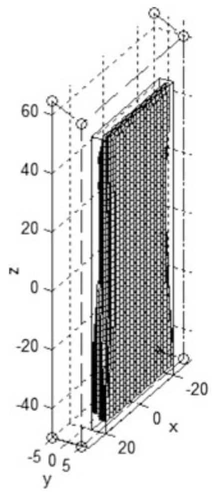

Fig. 4 IFWFW.

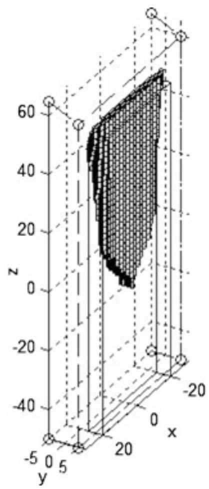

Fig. 5 IFWFW.

mobile platform was raised by more than a factor 5 in all directions. Although this had no real effect on the total stiffness of the mobile platform, since this is mostly determined by the very taut cables (e.g. Cable 3), it does mean that Cable 5 will be less influenced by outside factors like wind.

Using all the found data, the IFWFW can be calculated. In principle this is a 6 dimensional space, but to make the results presentable, three-dimensional IFWFWs are calculated for fixed sets of the vector θ. The grid for r is $40 \times 5 \times 100$ m in x, y and z direction respectively. Plotted are all the positions that point H can reach. Figure 4 shows the IFWFW for all rotations equal to zero. For 82% of the investigated grid points, the wrench was feasible and there was no interference. Figure 5 shows the IFWFW for a rotation of 45° around x_F. The cables interfere in the bottom part of the grid, but this rotation can be used to reach higher with point H. Now, 40% of the grid points were wrench feasible and interference free. For poses towards the core of the IFWFW, maximal surface interaction forces far higher than 100 N can be produced, e.g. 3.7 kN for $\mathbf{x} = [0,0,0,0°,0°,0°]^{\mathrm{T}}$.

The found IFWFW conforms rather well to a flat box-like shape, which is a good shape for cleaning building facades. To achieve this shape, the pulleys had to be positioned at quite a distance away from its edges. As long as this is not a problem, the CDPM is a viable option for a facade cleaning device. Within the workspace the mechanism is independent of surface features, but interference of cables with the surface still needs to be checked.

5 Discussion and Conclusion

In this paper, the occurrence of interference was defined as a limit to the workspace.

However, even after interference has occurred between cables or with the surface, the mechanism might still be able to function. This could favorably increase the workspace of e.g. the situation in Fig. 5. The assumption of interference between cable pairs resulted in an interference calculation method fast enough to be used in real-time operation. This method should not only work for the flat box-like CDPM configuration presented here, but also for similar configurations with different box shapes and sizes. These could be used to clean solar panel arrays or cooling towers.

It can be concluded that a CDPM is suitable for interaction with a large surface. Within the workspace, this surface can have any shape. A method has been developed in which linear cable theory is used to analyze cable interference and wrench feasibility for an over-actuated CDPM while taking into account the effects of cable mass. This method can be used to design CDPMs for surface interaction, which was done for a facade cleaning application. The designed mechanism is viable for this application as long as the pulleys can be placed at sufficient distances from the surface.

References

1. Diao, X., Ma, O.: Workspace determination of general 6-d.o.f. cable manipulators. Adv. Robot. **22**(2), 261–278 (2008)
2. Dornier, I.: Brush cleaning head. U.S. Patent WO 98/461121998
3. Elkmann, N., Felsch, T., Sack, M., Saenz, J., Hortig, J.: Innovative service robot systems for facade cleaning of difficult-to-access areas. In: IEEE International Conference on Intelligent Robots and Systems, pp. 756–762 (2002)
4. Gambao, E., Hernando, M., Hernández, F., Pinilla, E.: Cost-effective robots for façade cleaning. In: Proceedings of the 21st ISARC (2004)
5. Gouttefarde, M., Gosselin, C.: Analysis of the wrench-closure workspace of planar parallel cable-driven mechanisms. IEEE Trans. Robot. **22**(3), 343–445 (2006)
6. Gouttefarde, M., Merlet, J.P., Daney, D.: Wrench-feasible workspace of parallel cable-driven mechanisms. In: IEEE International Conference on Robotics and Automation, pp. 1492–1497 (2007)
7. Kozak, K.: Static analysis of cable-driven manipulators with non-negligible cable mass. IEEE Trans. Robot. **22**(3), 425–433 (2006)
8. Merlet, J.P.: Analysis of the influence of wires interference on the workspace of wire robots. In: Lenarčič, J., Galletti, C. (eds.) Advances in Robot Kinematics, pp. 211–218. Kluwer (2004)
9. Merlet, J.P.: Parallel Robots, 2nd edn. Springer, Dordrecht (2006)
10. Otis, M.J.D., Perreault, S., Nguyen-Dang, T.-L., Lambert, P., Gouttefarde, M., Laurendeau, D., Gosselin, C.: Determination and management of cable interferences between two 6-dof foot platforms in a cable-driven locomotion interface. IEEE Trans. Syst. Man Cybern., Part A, Syst. Humans **39**(3), 528–544 (2009)
11. Riechel, A.T., Ebert-Uphoff, I.: Force-feasible workspace analysis for underconstrained, point-mass cable robots. In: IEEE International Conference on Robotics and Automation, pp. 4956–4962 (2004)
12. Riehl, N., Gouttefarde, M., Baradat, C., Pierrot, F.: On the determination of cable characteristics for large dimension cable-driven parallel mechanisms. In: IEEE International Conference on Robotics and Automation, pp. 4709–4714 (2010)
13. Schraft, R.D., Bräuning, U., Orlowski, T., Hornemann, M.: Automated cleaning of windows on standard facades. Autom. Constr. **9**(5–6), 489–501 (2000)